US011780465B2

(12) **United States Patent**
Gummadi et al.

(10) **Patent No.: US 11,780,465 B2**
(45) **Date of Patent: *Oct. 10, 2023**

(54) **SYSTEM AND METHOD FOR FREE SPACE ESTIMATION**

(71) Applicant: **DEKA Products Limited Partnership**, Manchester, NH (US)

(72) Inventors: **Raajitha Gummadi**, Manchester, NH (US); **Christopher C. Langenfeld**, Nashua, NH (US); **Michael J. Slate**, Merrimack, NH (US); **Christopher J. Principe**, Nahant, MA (US)

(73) Assignee: **DEKA Products Limited Partnership**, Manchester, NH (US)

(*) Notice: Subject to any disclaimer, the term of this patent is extended or adjusted under 35 U.S.C. 154(b) by 0 days.

This patent is subject to a terminal disclaimer.

(21) Appl. No.: **17/951,331**

(22) Filed: **Sep. 23, 2022**

(65) **Prior Publication Data**

US 2023/0016896 A1 Jan. 19, 2023

Related U.S. Application Data

(63) Continuation of application No. 16/925,855, filed on Jul. 10, 2020, now Pat. No. 11,455,806.
(Continued)

(51) **Int. Cl.**
G06K 9/00 (2022.01)
B60W 60/00 (2020.01)
(Continued)

(52) **U.S. Cl.**
CPC ***B60W 60/0011*** (2020.02); ***G05D 1/0088*** (2013.01); ***G05D 1/0251*** (2013.01); ***G06F 18/2415*** (2023.01); ***G06T 7/33*** (2017.01); ***G06V 10/7715*** (2022.01); ***G06V 20/58*** (2022.01); ***G06V 20/588*** (2022.01);
(Continued)

(58) **Field of Classification Search**
CPC .. G06V 20/58; G06V 20/588; G06V 2201/12; G05D 1/0088; G05D 1/0251; G05D 2201/0213; G06K 9/6277; G06K 9/6232; G06T 7/33; G06T 2207/10028; G06T 2207/30256; G06T 2207/30261;
(Continued)

(56) **References Cited**

U.S. PATENT DOCUMENTS

10,839,530 B1 11/2020 Berger et al.
10,921,817 B1 2/2021 Kangaspunta
(Continued)

OTHER PUBLICATIONS

Written Opinion dated Nov. 12, 2020, issued in PCT International Patent Application No. PCT/US2020/043601, 8 pages.
(Continued)

Primary Examiner — Dhaval V Patel
(74) *Attorney, Agent, or Firm* — William A. Bonk, III

(57) **ABSTRACT**

A system and method for estimating free space including applying a machine learning model to camera images of a navigation area, where the navigation area is broken into cells, synchronizing point cloud data from the navigation area with the processed camera images, and associating probabilities that the cell is occupied and object classifications of objects that could occupy the cells with cells in the navigation area based on sensor data, sensor noise, and the machine learning model.

25 Claims, 11 Drawing Sheets

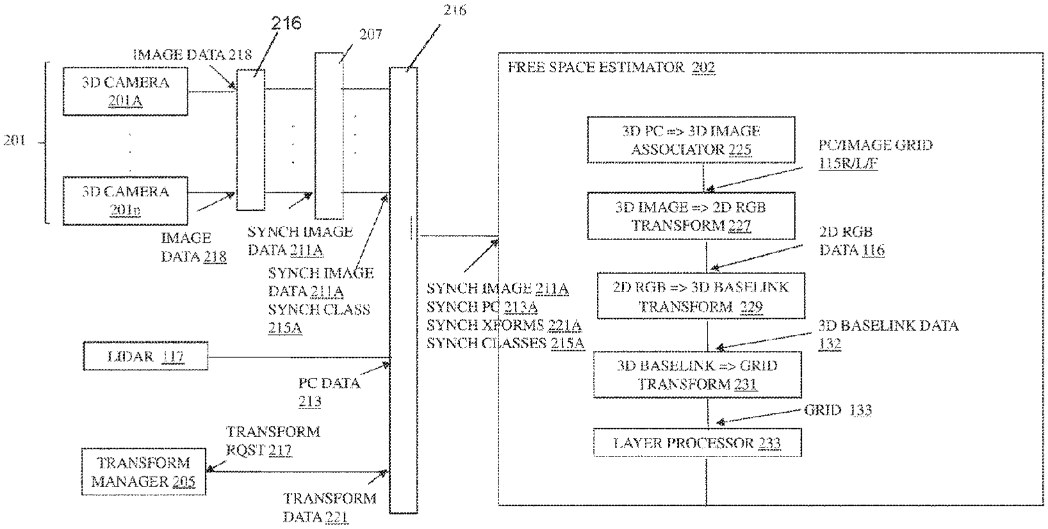

Related U.S. Application Data

(60) Provisional application No. 62/872,583, filed on Jul. 10, 2019.

(51) **Int. Cl.**

G06T 7/33	(2017.01)
G05D 1/00	(2006.01)
G05D 1/02	(2020.01)
G06V 20/58	(2022.01)
G06V 20/56	(2022.01)
G06F 18/2415	(2023.01)
G06V 10/77	(2022.01)
G01S 17/894	(2020.01)

(52) **U.S. Cl.**
CPC *G01S 17/894* (2020.01); *G05D 2201/0213* (2013.01); *G06T 2207/10028* (2013.01); *G06T 2207/30256* (2013.01); *G06T 2207/30261* (2013.01)

(58) **Field of Classification Search**
CPC G01S 17/894; G01S 17/87; G01S 17/89; G01S 17/931; B60W 60/0011
See application file for complete search history.

(56) **References Cited**

U.S. PATENT DOCUMENTS

10,970,871	B2	4/2021	Nezhadarya et al.	
11,004,202	B2	5/2021	Tchapmi et al.	
11,004,261	B2	5/2021	Yao et al.	
11,062,454	B1	7/2021	Cohen et al.	
11,537,139	B2 *	12/2022	Rankawat	G06V 20/58
2018/0101720	A1 *	4/2018	Liu	G06V 20/647
2018/0196139	A1 *	7/2018	Brown	G01S 17/10
2019/0188541	A1 *	6/2019	Wang	G01C 3/08
2019/0324148	A1 *	10/2019	Kim	G01S 17/89
2020/0191971	A1	6/2020	Hua et al.	
2021/0012120	A1	1/2021	Gummadi et al.	
2021/0373161	A1	12/2021	Lu et al.	

OTHER PUBLICATIONS

Borgmann et al., Usage of Multiple LiDAR Sensors on a Mobile System for the Detection of Persons with Implicit Shape Models, The International Archives of the Photogrammetry, Remote Sensing an Spatial Information Sciences, vol. XLII-2, 2018, Jun. 4-7, 2018, Italy, 7 pages.

Chen et al., Transforming a 3-D LiDAR Point Cloud Into a 2-D Dense Depth Map Through a Parameter Self-Adaptive Framework, IEEE Transactions of the Intelligent Transportation Systems, IEEE Transactions on Intelligent Transportation Systems, vol. 18:1, pp. 165-176, 12 pages, Jan. 2017.

Choy et al., Enriching Object Detection with 2D-3D Registration and Continuous Viewpoint Estimation, 2015 IEEE Conference on Computer Vision and Pattern Recognition (CVPR), pp. 2512-2520, 9 pages, 2015.

De Silva et al., Robust Fusion of LiDAR and Wide-Angle Camera Data for Autonomous Mobile Robots, Institute for Digital Technologies, Loughborough University, London E15 2GZ, Uk, Aug. 20, 2018, 21 pages.

Harakeh, Towards Fully Self-Supervised Free Space Estimation for Unmanned Ground Vehicles, A Thesis, American University of Beirut, Beirut, Lebanon, Apr. 2016, 58 pages.

Harms et al., Grid Map based Free Space Estimation using Stereo Vision, Institute of Measurement and Control Systems, Karlsruhe Institute of Technology, Karlsruhe Germany, 2015, 2 pages.

He et al., A Novel Way to Organize 3D LiDAR Point Cloud as 2D Depth Map Height Map and Surface Normal Map, 2015 IEEE International Conference on Robotics and Biomimetics (ROBIO), pp. 1383-1388, Dec. 6-9, 2015, 6 pages.

Huang et al., A Practical Point Cloud Based Road Curb Detection Method for Autonomous Vehicle, sss.mdpi.com/journal/information, Information 2017, 8, 93, Jul. 30, 2017, 24 pages.

Kim et al., Design and Implementation of Ground Plane Detection using Predefined Datasets and Space Geometric Analysis, Journal of Semiconductor Technology and Science, vol. 18, No. 4, Aug. 2018, 9 pages.

Kocić et al., Sensors and Sensor Fusion in Autonomous Vehicles, 2018 26th Telecommunications Forum (TELFOR), Nov. 20-21, pp. 420-425, 2018, 5 pages.

Li et al., Light-Head R-CNN: In Defense of Two-Stage Object Detector, arXiv: 1711.07264 [cs.CV], Nov. 23, 2017, 9 pages.

Open CV, Open Source Computer Vision—Camera Calibration with Open CV, doxygen, Mar. 29, 2019, https://docs.opencv.org/3.4.6/d4/d94/tutorial_camera_calibration.html, 16 pages.

ROS.org, How to Calibrate a Monocular Camera, Open Source Robotics Foundation, Apr. 20, 2017, http://wiki.ros.org/camera calibration/Tutorials/MonocularCalibration, 8 pages.

Park et al., Calibration between Color Camera and 3D LiDAR Instruments with a Polygonal Planar Board, Sensors ISSN 1424-8220, vol. 14:5333-5353, Mar. 17, 2014, 21 pages.

Rodríguez-Cuenca et al., Morphological Operations to Extract Urban Curbs in 3D MLS Point Clouds, International Journal of Geo-Information, Jun. 14, 2016, 17 pages.

Sahdev, Free Space Estimation using Occupancy Grids and Dynamic Object Detection, arXiv:1708.04989 [cs.CV], https://arxiv.org/abs/1708.04989, Aug. 16, 2017, 10 pages.

Free_Space_Estimation_for_Autonomous_Navigation, 2007, Bielefeld, Germany, 11 pages.

Velas et al., Calibration of RGB Camera with Velodyne LiDAR, WSCG2014 Conference on Computer Graphics, Visualization and Computer Vision, 2014, 10 pages.

Velodyne LiDAR-VLP-32C User Manual 63-9325 Rev. B, 2018, 136 pages.

Wang, Semantic Segmentation, Machine Learning Group, University of Toronto, https://www.cs.toronto.edu/~tingwuwang/semantic_segmentation.pdf, 2017.

Xiao et al., Gaussian process regression-based robust free space detection for autonomous vehicle by 3-D point cloud and 2-D appearance information fusion, International Journal of Advanced Robotic Systems, Jul.-Aug. 2017, 20 pages.

Yao et al., Estimating Drivable Collision-Free Space for Monocular Video, Mitsubishi Electric Research Laboratories, IEEE Winter Conference on Applications of Computer Vision, pp. 420-427, Jan. 6, 2015, 9 pages.

* cited by examiner

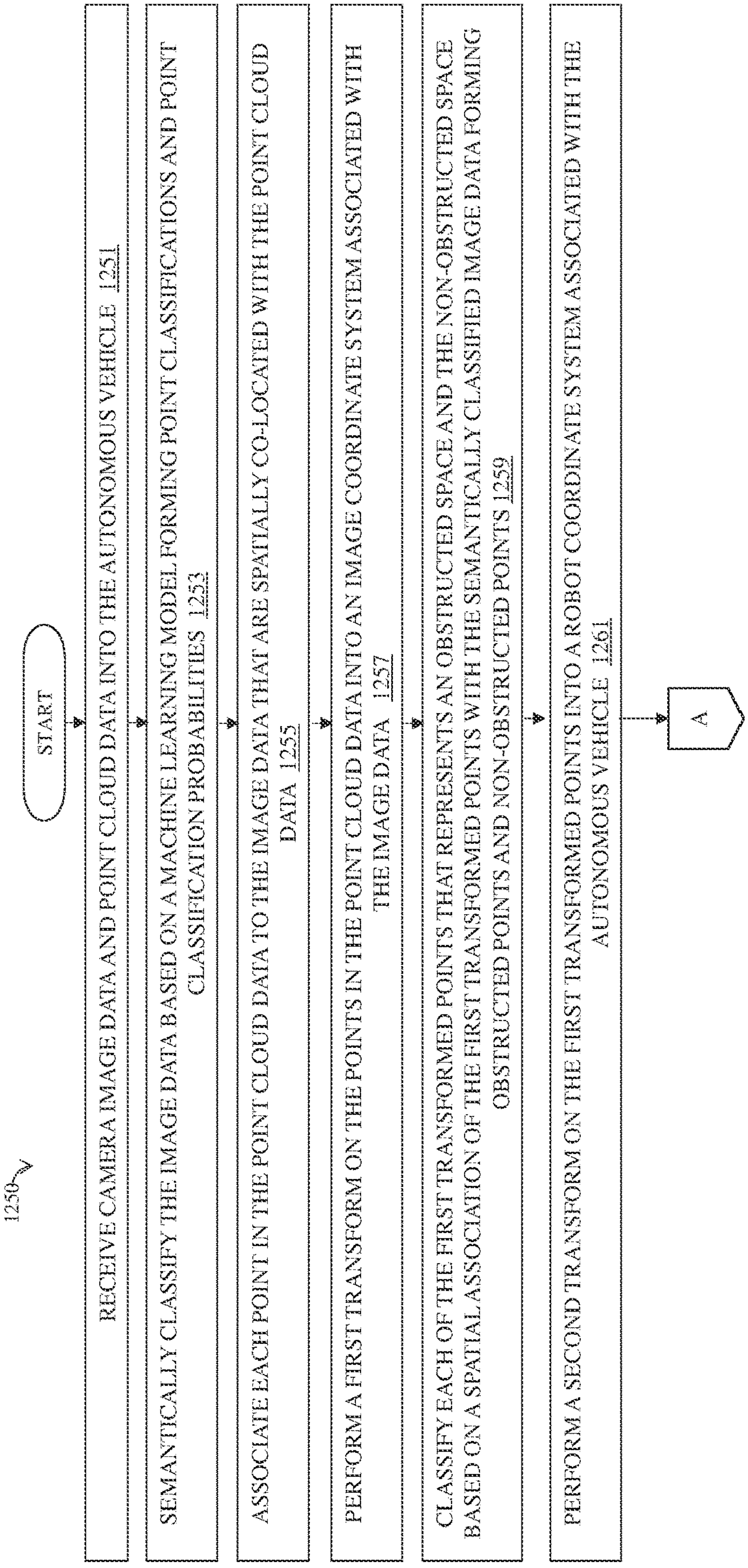
1250
START
RECEIVE CAMERA IMAGE DATA AND POINT CLOUD DATA INTO THE AUTONOMOUS VEHICLE 1251
SEMANTICALLY CLASSIFY THE IMAGE DATA BASED ON A MACHINE LEARNING MODEL FORMING POINT CLASSIFICATIONS AND POINT CLASSIFICATION PROBABILITIES 1253
ASSOCIATE EACH POINT IN THE POINT CLOUD DATA TO THE IMAGE DATA THAT ARE SPATIALLY CO-LOCATED WITH THE POINT CLOUD DATA 1255
PERFORM A FIRST TRANSFORM ON THE POINTS IN THE POINT CLOUD DATA INTO AN IMAGE COORDINATE SYSTEM ASSOCIATED WITH THE IMAGE DATA 1257
CLASSIFY EACH OF THE FIRST TRANSFORMED POINTS THAT REPRESENTS AN OBSTRUCTED SPACE AND THE NON-OBSTRUCTED SPACE BASED ON A SPATIAL ASSOCIATION OF THE FIRST TRANSFORMED POINTS WITH THE SEMANTICALLY CLASSIFIED IMAGE DATA FORMING OBSTRUCTED POINTS AND NON-OBSTRUCTED POINTS 1259
PERFORM A SECOND TRANSFORM ON THE FIRST TRANSFORMED POINTS INTO A ROBOT COORDINATE SYSTEM ASSOCIATED WITH THE AUTONOMOUS VEHICLE 1261
A

FIG. 1A

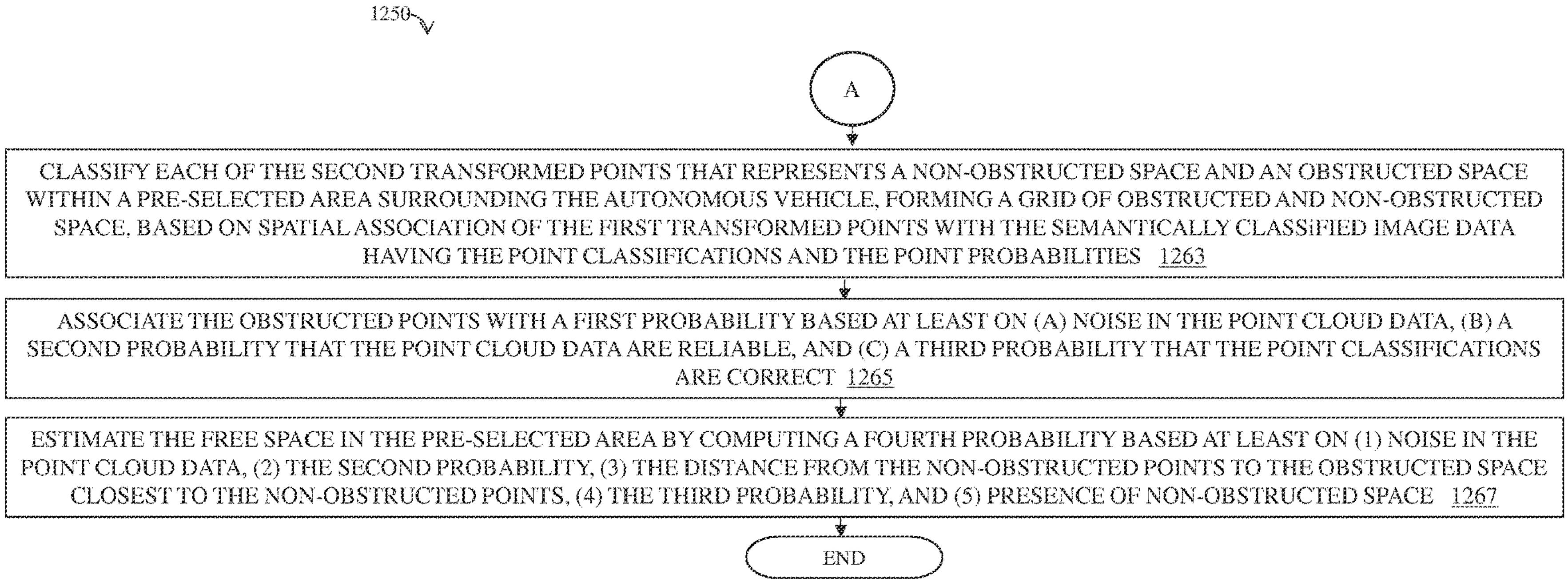

CLASSIFY EACH OF THE SECOND TRANSFORMED POINTS THAT REPRESENTS A NON-OBSTRUCTED SPACE AND AN OBSTRUCTED SPACE WITHIN A PRE-SELECTED AREA SURROUNDING THE AUTONOMOUS VEHICLE, FORMING A GRID OF OBSTRUCTED AND NON-OBSTRUCTED SPACE, BASED ON SPATIAL ASSOCIATION OF THE FIRST TRANSFORMED POINTS WITH THE SEMANTICALLY CLASSIFIED IMAGE DATA HAVING THE POINT CLASSIFICATIONS AND THE POINT PROBABILITIES 1263

ASSOCIATE THE OBSTRUCTED POINTS WITH A FIRST PROBABILITY BASED AT LEAST ON (A) NOISE IN THE POINT CLOUD DATA, (B) A SECOND PROBABILITY THAT THE POINT CLOUD DATA ARE RELIABLE, AND (C) A THIRD PROBABILITY THAT THE POINT CLASSIFICATIONS ARE CORRECT 1265

ESTIMATE THE FREE SPACE IN THE PRE-SELECTED AREA BY COMPUTING A FOURTH PROBABILITY BASED AT LEAST ON (1) NOISE IN THE POINT CLOUD DATA, (2) THE SECOND PROBABILITY, (3) THE DISTANCE FROM THE NON-OBSTRUCTED POINTS TO THE OBSTRUCTED SPACE CLOSEST TO THE NON-OBSTRUCTED POINTS, (4) THE THIRD PROBABILITY, AND (5) PRESENCE OF NON-OBSTRUCTED SPACE 1267

FIG. 1B

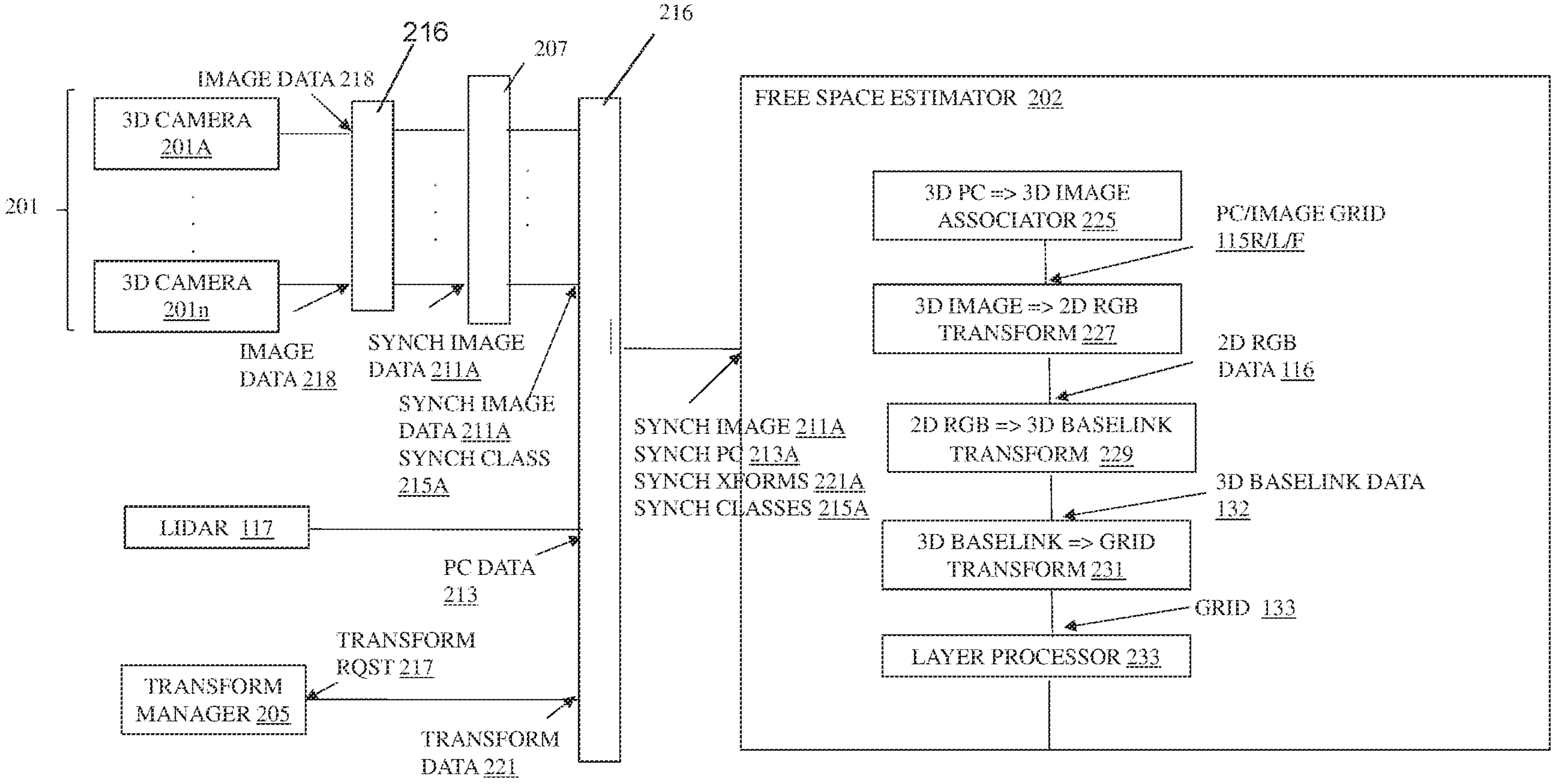

201
3D CAMERA 201A
3D CAMERA 201n
IMAGE DATA 218
IMAGE DATA 218
216
207
216
SYNCH IMAGE DATA 211A
SYNCH IMAGE DATA 211A
SYNCH CLASS 215A
LIDAR 117
PC DATA 213
TRANSFORM MANAGER 205
TRANSFORM RQST 217
TRANSFORM DATA 221
SYNCH IMAGE 211A
SYNCH PC 213A
SYNCH XFORMS 221A
SYNCH CLASSES 215A
FREE SPACE ESTIMATOR 202
3D PC => 3D IMAGE ASSOCIATOR 225
PC/IMAGE GRID 115R/L/F
3D IMAGE => 2D RGB TRANSFORM 227
2D RGB DATA 116
2D RGB => 3D BASELINK TRANSFORM 229
3D BASELINK DATA 132
3D BASELINK => GRID TRANSFORM 231
GRID 133
LAYER PROCESSOR 233

FIG. 2

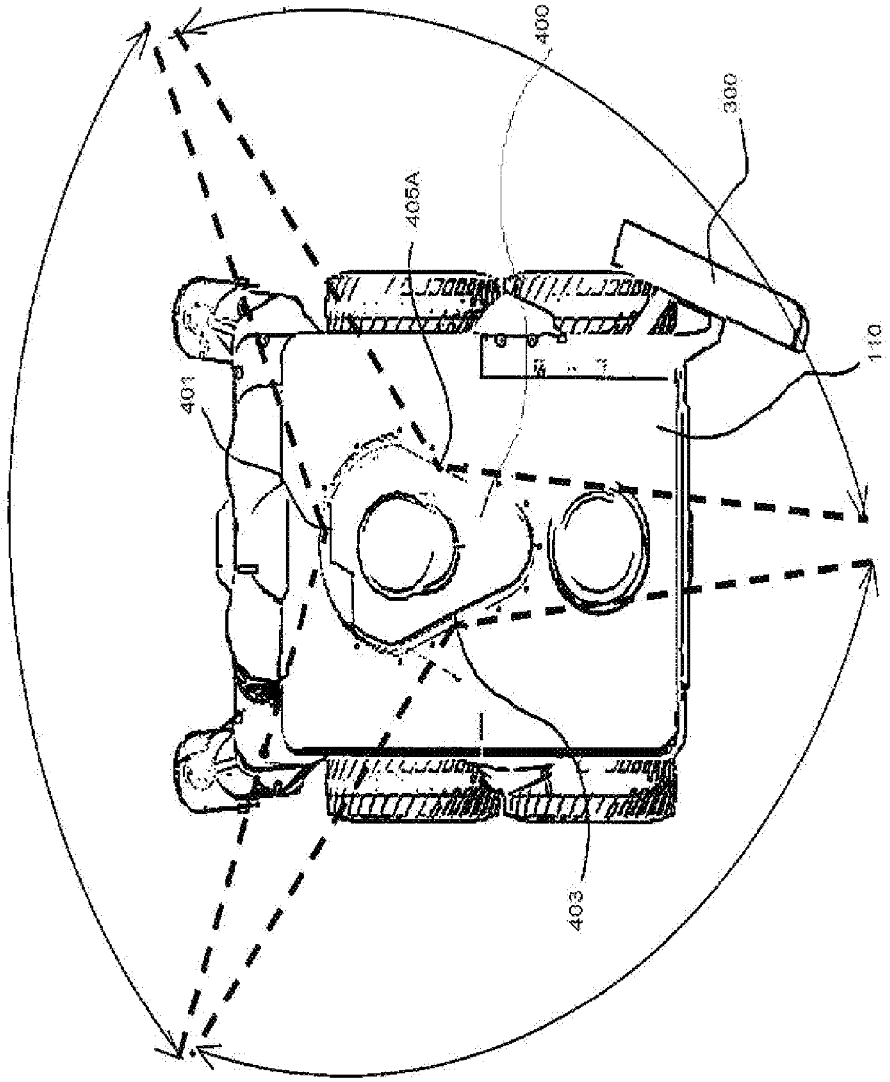

FIG. 2A

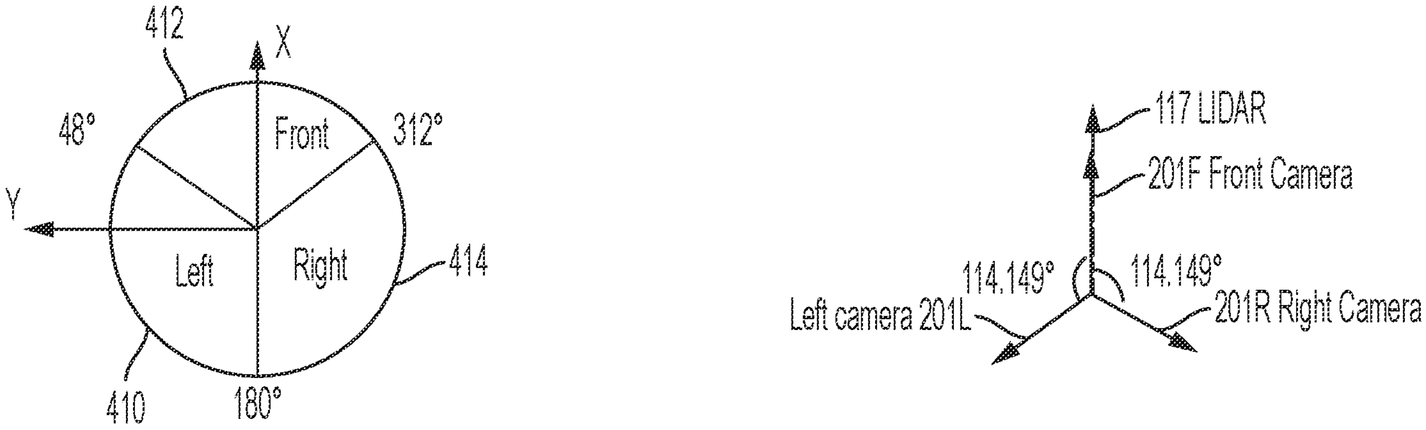
412
X
48°
Front
312°
Y
Left
Right
414
410
180°
117 LIDAR
201F Front Camera
114.149°
114.149°
Left camera 201L
201R Right Camera

FIG. 2B

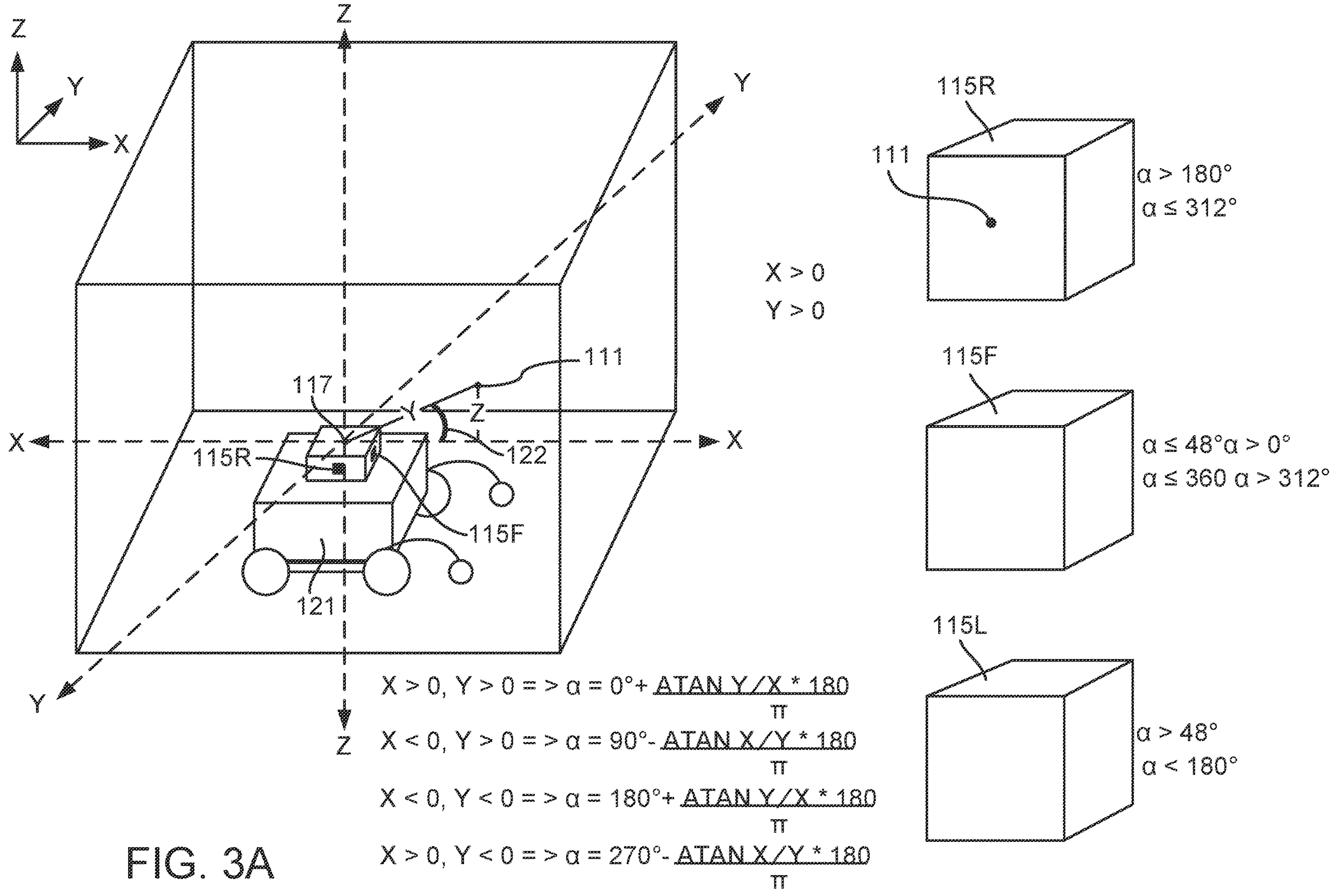

$$X > 0, Y > 0 => \alpha = 0° + \frac{\underline{ATAN\ Y/X * 180}}{\pi}$$

$$X < 0, Y > 0 => \alpha = 90° - \frac{\underline{ATAN\ X/Y * 180}}{\pi}$$

$$X < 0, Y < 0 => \alpha = 180° + \frac{\underline{ATAN\ Y/X * 180}}{\pi}$$

$$X > 0, Y < 0 => \alpha = 270° - \frac{\underline{ATAN\ X/Y * 180}}{\pi}$$

FIG. 3A

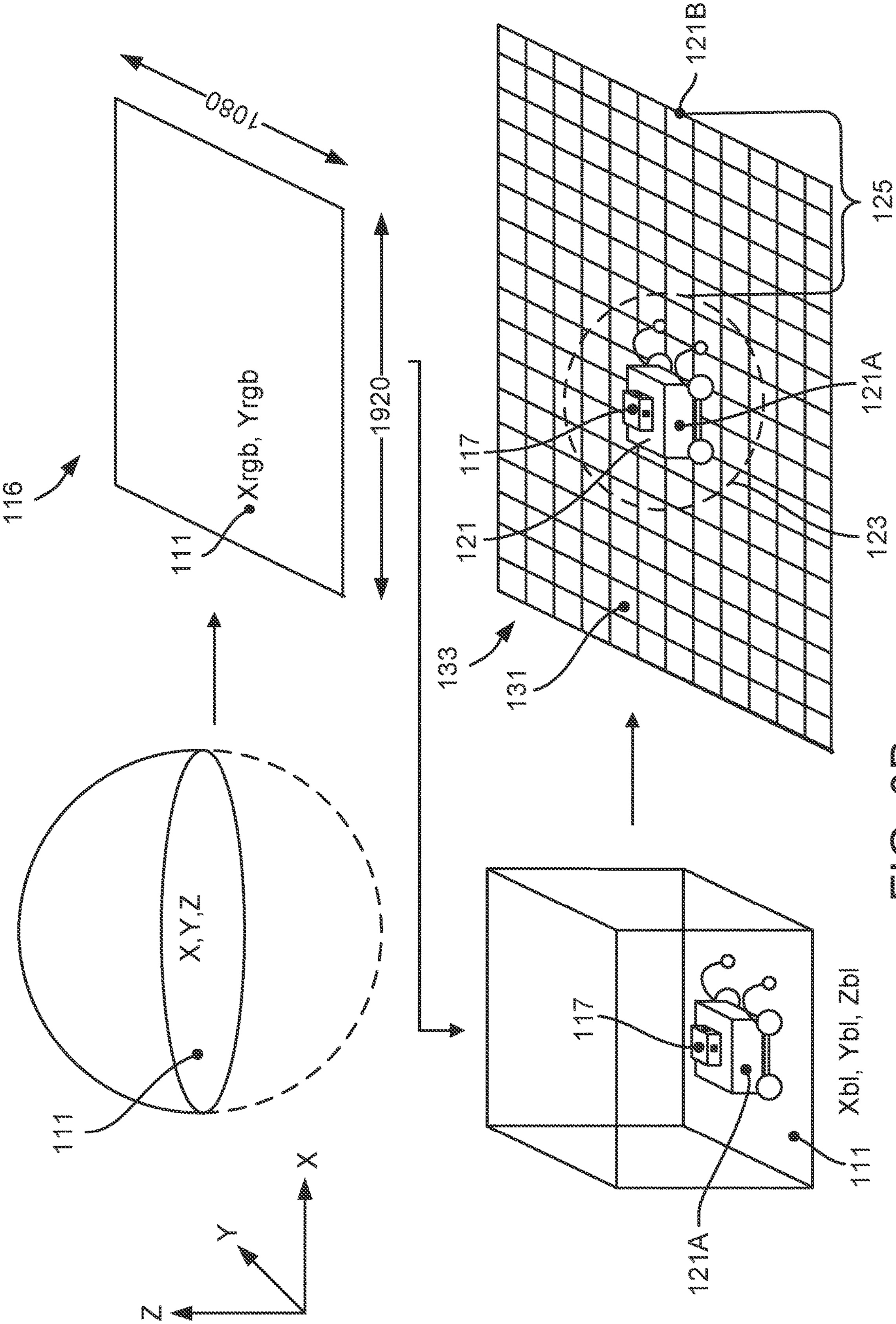
116
1080
1920
Xrgb, Yrgb
111
121B
125
117
121A
121
123
133
131
X,Y,Z
111
117
Xbl, Ybl, Zbl
111
121A
X
Y
Z

FIG. 3B

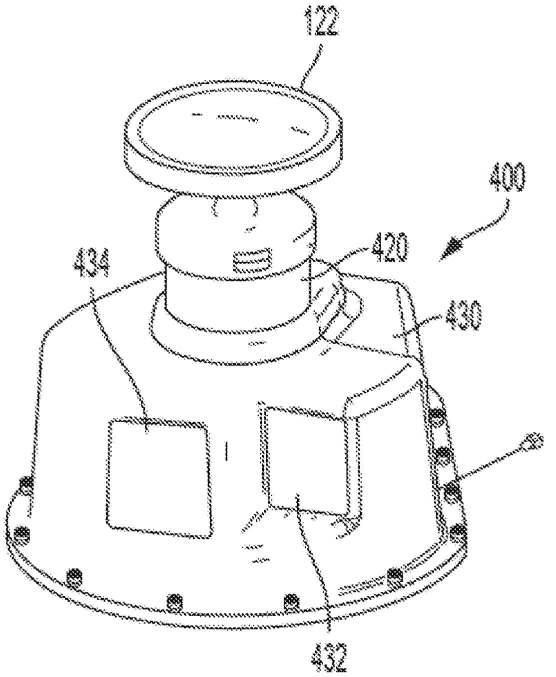

FIG. 4A

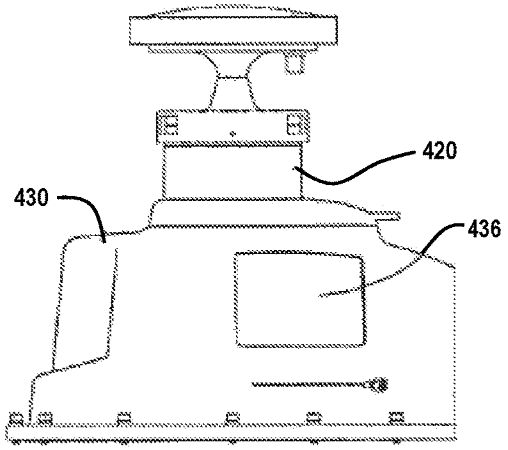

FIG. 4B

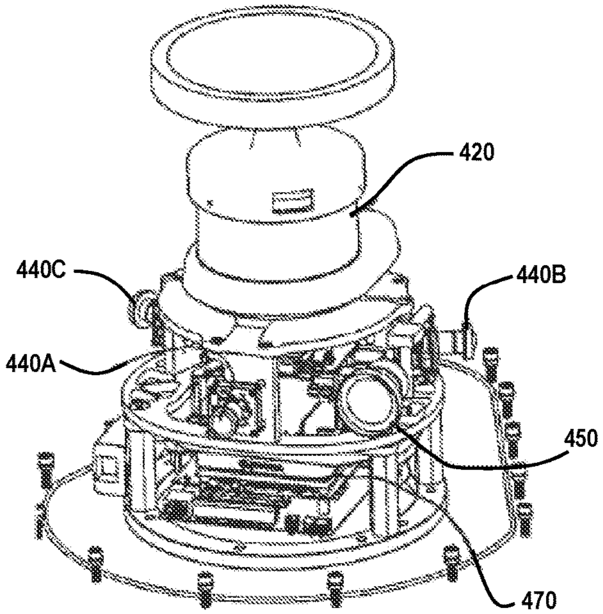

FIG. 4C

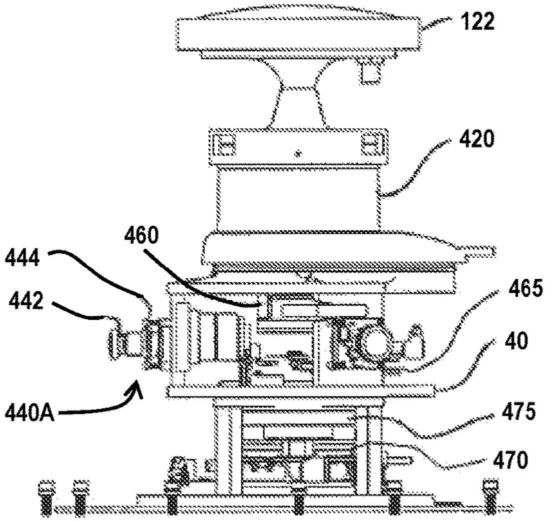

FIG. 4D

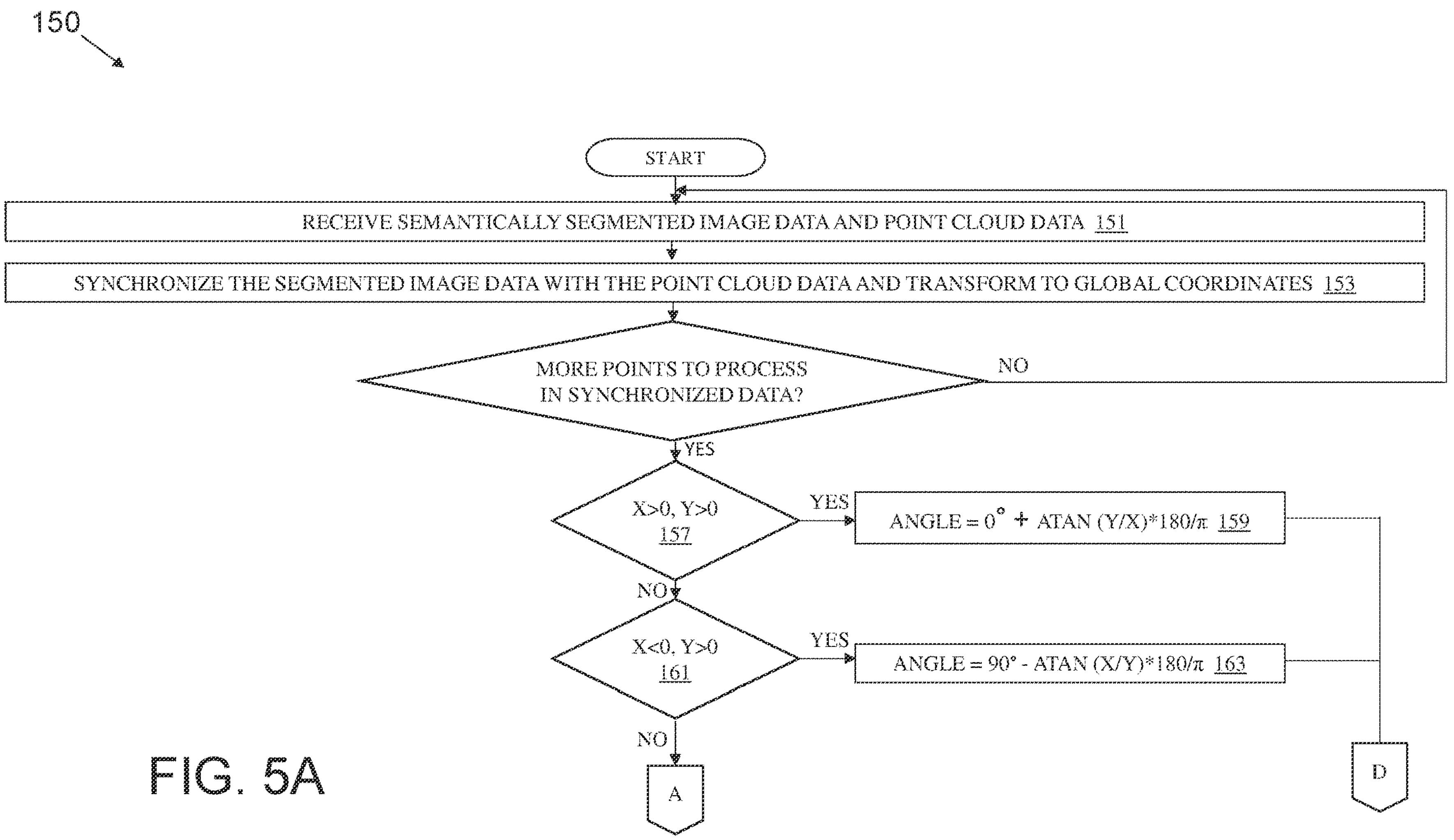
150
START
RECEIVE SEMANTICALLY SEGMENTED IMAGE DATA AND POINT CLOUD DATA 151
SYNCHRONIZE THE SEGMENTED IMAGE DATA WITH THE POINT CLOUD DATA AND TRANSFORM TO GLOBAL COORDINATES 153
MORE POINTS TO PROCESS IN SYNCHRONIZED DATA?
NO
YES
X>0, Y>0 157
YES
ANGLE = 0° + ATAN (Y/X)*180/π 159
NO
X<0, Y>0 161
YES
ANGLE = 90° - ATAN (X/Y)*180/π 163
NO
A
D

FIG. 5A

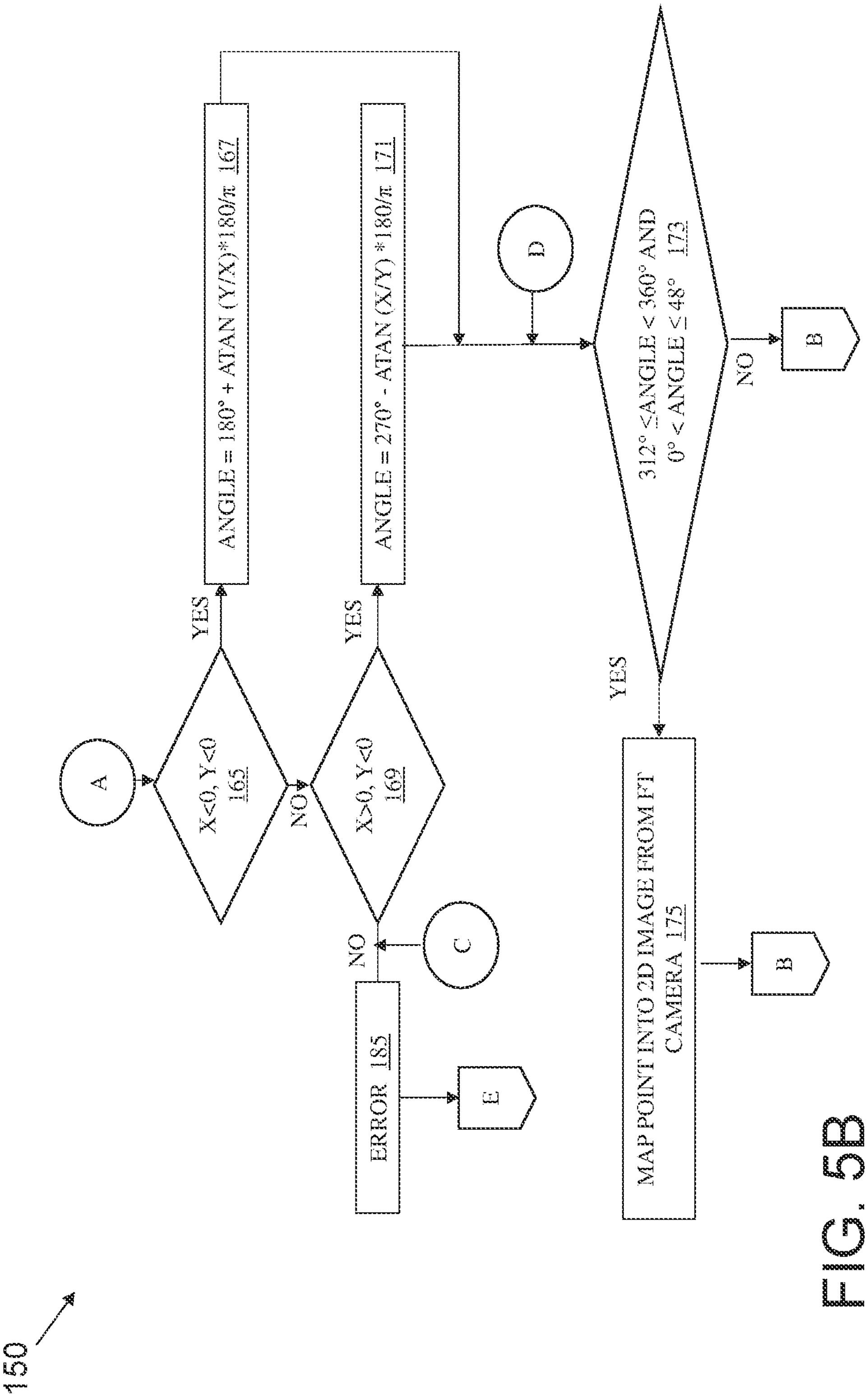
150
A
X<0, Y<0
165
YES
ANGLE = 180° + ATAN (Y/X)*180/π 167
NO
X>0, Y<0
169
YES
ANGLE = 270° - ATAN (X/Y) *180/π 171
NO
C
ERROR 185
E
D
312° ≤ANGLE < 360° AND
0° < ANGLE ≤ 48° 173
NO
B
YES
MAP POINT INTO 2D IMAGE FROM FT
CAMERA 175
B

FIG. 5B

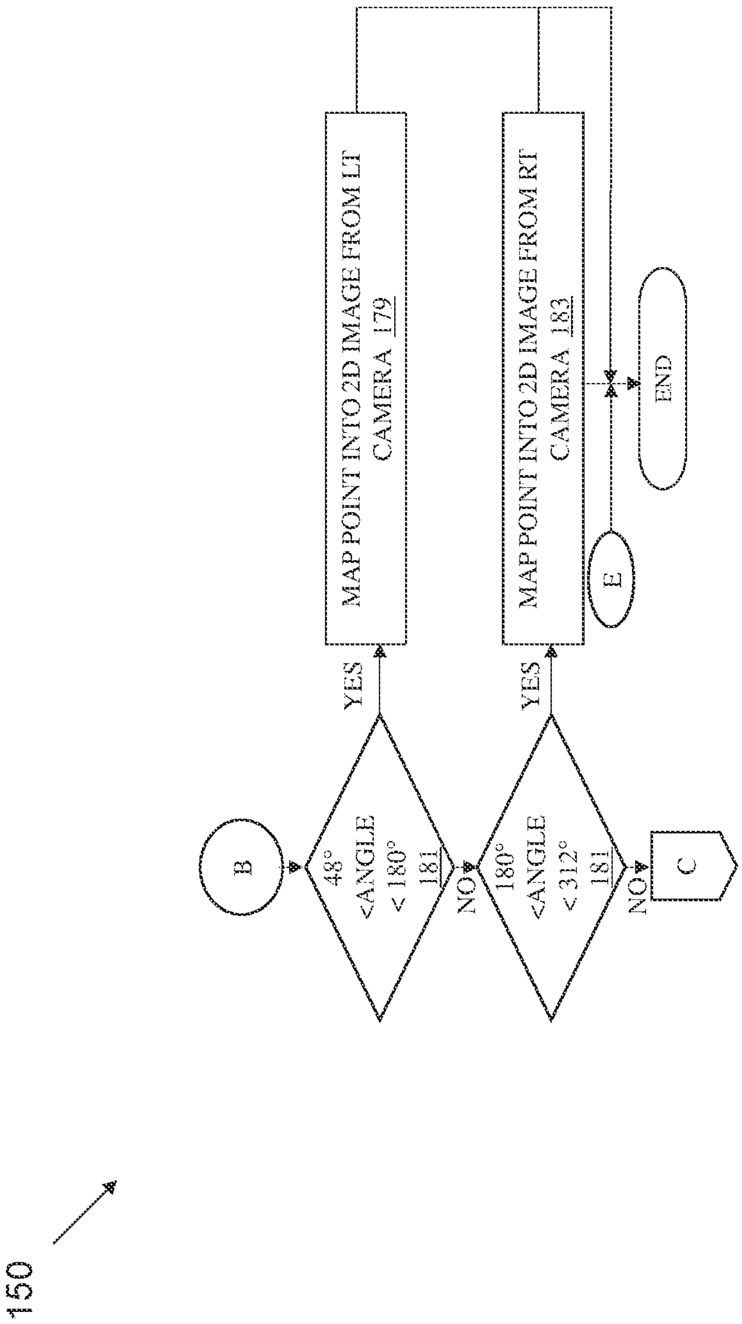
B
48° <ANGLE < 180° 181
YES
MAP POINT INTO 2D IMAGE FROM LT CAMERA 179
NO
180° <ANGLE < 312° 181
YES
MAP POINT INTO 2D IMAGE FROM RT CAMERA 183
NO
C
E
END
150

FIG. 5C

SYSTEM AND METHOD FOR FREE SPACE ESTIMATION

CROSS REFERENCE TO RELATED APPLICATIONS

This utility patent application is a continuation of U.S. patent application Ser. No. 16/925,855 filed Jul. 10, 2020, entitled System and Method for Free Space Estimation, now U.S. Pat. No. 11,455,806, issued Sep. 27, 2022 which claims the benefit of U.S. Provisional Patent Application Ser. No. 62/872,583 filed Jul. 10, 2019, entitled System and Method for Free Space Estimation, all of which are incorporated herein by reference in their entirety.

BACKGROUND

Various methods for organizing 3D LIDAR point cloud data as a 2D depth map, height map, and surface normal map exist. What is needed is a system that applies a machine learning model to camera images of a navigation area, where the navigation area is broken into cells, synchronizes point cloud data from the navigation area with the processed camera images, and associates probabilities that the cell is occupied and object classifications of objects that could occupy the cells with cells in the navigation area based on sensor data, sensor noise, and the machine learning model.

SUMMARY

The method of the present teachings for estimating free space based on image data and point cloud data, the free space used for navigating an autonomous vehicle, the method can include, but is not limited to including, receiving camera image data and point cloud data into the autonomous vehicle, semantically classifying the image data based on a machine learning model forming point classifications and point classification probabilities, and associating each point in the point cloud data to the image data that are spatially co-located with the point cloud data. The method can include performing a first transform on the points in the point cloud data into an image coordinate system associated with the image data and classifying each of the first transformed points that represents an obstructed space and the non-obstructed space based on a spatial association of the first transformed points with the semantically classified image data forming obstructed points and non-obstructed points. The method can include performing a second transform on the first transformed points into a robot coordinate system associated with the autonomous vehicle, and classifying each of the second transformed points that represents a non-obstructed space and an obstructed space within a pre-selected area surrounding the autonomous vehicle. The classifying can form a grid of obstructed and non-obstructed space based on spatial association of the first transformed points with the semantically classified image data having the point classifications and the point probabilities. The method can include associating the obstructed points with a first probability based at least on (a) noise in the point cloud data, (b) a second probability that the point cloud data are reliable, and (c) a third probability that the point classifications are correct, and estimating the free space in the pre-selected area by computing a fourth probability based at least on (1) noise in the point cloud data, (2) the second probability, (3) the distance from the non-obstructed points to the obstructed space closest to the non-obstructed points, (4) the third probability, and (5) presence of non-obstructed space.

The camera image data can optionally include streaming data from a pre-selected number of cameras, the at least one camera providing a 360° view of an area surrounding the autonomous vehicle. The at least one camera can optionally include providing the image data through a MIPI interface at a pre-selected resolution. The pre-selected resolution can optionally include 2180×720 pixels. The machine learning model can optionally include an ICNET semantic segmentation model. The machine learning model can optionally include detecting at least one drivable surface. The at least one drivable surface can optionally include road, sidewalk, ground, terrain surfaces, and lane markings. The associating each point can optionally include receiving the image data at a pre-selected rate, and mapping the point cloud data onto the image data.

The system of the present teachings for estimating free space based on image data and point cloud data, where the free space can be used for navigating an autonomous vehicle, and where the autonomous vehicle can include a front, a left side, and a right side, the system can include, but is not limited to including, a pre-processor receiving camera image data from at least one camera into the autonomous vehicle. The pre-processor can semantically classify each pixel of the image data into a classification, and can calculate a probability associated with the classification. The classification and the probability can be determined by a machine learning model. The system can include a free space estimator that can include, but is not limited to including, a 3D point cloud to 3D image processor transforming the 3D point cloud to 3D image coordinates, a 3D image to 2D RGB transform transforming the 3D image coordinates to 2D RGB coordinates, a 2D to 3D baselink transform transforming the 2D RGB coordinates to 3D baselink coordinates, and a layer processor computing obstacle classification, probability, and log odds layers based on the processing point cloud and image data.

The camera image data can optionally include streaming data from at least one camera. The at least one camera can optionally provide a 360° view of an area surrounding the autonomous vehicle. The number of cameras can optionally include three or four. The machine learning model can optionally include detecting drivable surfaces, and the drivable surfaces can optionally include lane markings. The lane markings can optionally include solid white lines, broken white lines, yellow lines and cross walks, and can optionally indicate travel in the direction of the autonomous vehicle. The point cloud data can optionally include LIDAR data. The free space estimator can optionally include receiving data having time stamps into a synchronizer. The synchronizer can optionally include time-synchronizing the point cloud data, the transform data, and the classifications based on the time stamps. The time stamps can optionally include marking a time when a data block is acquired from a sensor or a transform manager. The 3D point cloud to 3D image processor can optionally include receiving the point cloud data from at least one LIDAR sensor, the classifications and the probabilities, and coordinate transforms, associating each point in the point cloud data to the image data that are spatially co-located with the point cloud data, and performing a first transform on the points in the point cloud data into an image coordinate system associated with the image data. The associating each point in the synchronized point cloud data with the synchronized image data can optionally include, for each point (X,Y,Z) in the synchronized point cloud data, calculating an angle that the point subtends with a center of the synchronized point cloud data, the angle indicating a field of view of the at least one camera. The calculating can optionally include, if X>0 and Y>0 then the angle=0°+atan(Y/X) degrees*180/π, if X<0 and Y>0 then the angle=90°−atan(X/Y) degrees*180/π, if X<0 and Y<0 then the angle=180°+atan(Y/X) degrees*180/π, and if X>0 and Y<0 then the angle=270°−atan(X/Y) degrees*180/π. The associating can optionally include mapping each point onto the semantic segmentation output image that can optionally include, if 312°<the angle≤360° or 48°≥the angle>0°, then mapping the point onto the semantic segmentation output image derived from the at least one camera located at the front of the autonomous vehicle, or, if 48°<the angle<180°, then mapping the point onto the semantic segmentation output image derived from the at least one camera located on the left side, and, if 180°<the angle≤312°, then mapping the point onto the semantic segmentation output image derived from the at least one camera located on the right side. The 3D image to 2D RGB transform can optionally include identifying each of the first transformed points that represents an obstructed space and a non-obstructed space based on a spatial association of the first transformed points with the semantically classified image data. The 2D to 3D baselink transform can optionally include performing a second transform on the first transformed points into a robot coordinate system associated with the autonomous vehicle. The 3D baselink to grid transform can optionally include flattening the robot coordinate system points (Xbl, Ybl, Zbl) to a 2D grid map surrounding the autonomous device. The 2D grid map can optionally extend to a pre-selected radius around the autonomous device. The 3D baselink to grid transform can optionally include identifying a cell of the 2D grip map as occupied if a semantic segmentation output point (XRGB, YRGB), of the semantic segmentation output image, spatially associated with the cell, corresponds to an obstructed space. The pre-selected radius can optionally include about 20 m. The semantic segmentation output point (XRGB, YRGB) can optionally include values including 0=non-drivable, 1=road, 2=sidewalk, 3=terrain, 4=lane marking, >0=drivable, 0=obstructed. The obstructed space can optionally include at least one surface being impassable by a vehicle. The vehicle can optionally include a wheelchair, a bicycle, or a car sized vehicle. The layer processor can optionally include classifying each of the second transformed points that represents a non-obstructed space and an obstructed space within a pre-selected area surrounding the autonomous vehicle. The classifying can optionally form a grid of obstructed and non-obstructed space, based on spatial association of the first transformed points with the semantically classified image data having the point classifications and the point probabilities. The layer processor can optionally include associating the obstructed points with a first probability based at least on (a) noise in the point cloud data, (b) a second probability that the point cloud data are reliable, and (c) a third probability that the point classifications are correct, and estimating the free space in the pre-selected area by computing a fourth probability based at least on (1) noise in the point cloud data, (2) the second probability, (3) the distance from the non-obstructed points to the obstructed space closest to the non-obstructed points, (4) the third probability, and (5) presence of non-obstructed space. The non-obstructed space can optionally include space that is not part of the obstructed space. The layer processor can optionally include estimating the free space by extending a line from a center of the grid map to the boundary of the pre-selected area, and, along the line, marking the free space as the cells that are not the obstructed space in the grid map between a blind area and the last free space present in the line. The blind area can optionally include an area surrounding the LIDAR sensor where the point cloud data cannot be gathered.

The method of the present teachings for mapping point cloud data from at least one LIDAR sensor onto semantically segmented image data from a plurality of cameras, the at least one LIDAR sensor and the plurality of cameras being located upon an autonomous vehicle, the method can include, but is not limited to including, accessing a synchronizer. The synchronizer can provide time synchronized point cloud data and the semantically segmented image data that are based on the time stamps on point cloud data and semantically segmented image data that are received simultaneously, forming time-synchronized point cloud data from the time stamped point cloud data and time-synchronized semantically segmented image data from the time stamped semantically segmented image data. The method can include receiving time-synchronized point cloud data and the time-synchronized semantically segmented image data from the plurality of cameras, the plurality of cameras being mounted on a front of the autonomous vehicle, on a left side of the autonomous vehicle, and on an opposing right side of the autonomous vehicle. The method can include translating the time-synchronized point cloud data from a LIDAR coordinate system associated with the at least one LIDAR sensor to an image coordinate system associated with the at least one camera. The translating can include applying a roll of −90° and a yaw of −90° to the point cloud data, the rotation producing rotated point cloud data in a 3D frame of reference according to a rotation matrix R, converting the LIDAR points associated with the aligned LIDAR frame of reference to 3D image points by applying the translation matrix R and camera translation factors tx/ty/tz to the rotated point cloud data, and applying camera rotation matrices r to the rotated point cloud data to align a LIDAR frame of reference of the at least one LIDAR sensors with a camera frame of reference associated with the at least one camera. The translating can include accessing a calibration matrix K associated with the at least one camera, applying the calibration matrix K to the 3D image points forming calibrated 3D image points (x,y,z), and converting the calibrated 3D image points (x,y,z) to 2D points (Xrgb,Yrgb) wherein Xrgb=x/z, Yrgb=y/z. The method can include providing each of 2D points (Xrgb,Yrgb) a depth value of a LIDAR point that is closest to the autonomous vehicle.

Computing the translation matrix R can optionally include computing Euler and Tait-Bryan rotations as a combined rotation matrix of 3-axis rotation matrices (Rx, Ry,Rz). The combined rotation matrix can be a product of two or three of the rotation matrices (Rx,Ry,Rz). Computing the translation matrices r can optionally include, for each point (X,Y,Z) in the point cloud data, calculating an angle that the point (X,Y,Z) subtends with a center of the LIDAR sensor. If X>0 and Y>0 then the angle=0°+atan(Y/X) degrees*180/π. If X<0 and Y>0 then the angle=90°−atan (X/Y) degrees*180/π. If X<0 and Y<0 then the angle=180°+atan(Y/X) degrees*180/π. If X>0 and Y<0 then the angle=270°−atan(X/Y) degrees*180/π. If 312°≤the angle≤360° or 48°≥the angle>0°, computing the translation matrices r can optionally include mapping the point (X,Y,Z) onto the semantic segmentation output image derived from the front camera. If the angle>48° and the angle<180°, computing the translation matrices r can optionally include mapping the point (X,Y,Z) onto the semantic segmentation output image derived from the left camera. If the angle>180° and angle≤312°, computing the translation matrices r can optionally include mapping the point (X,Y,Z) onto the semantic segmentation output image derived from the right camera. Computing the translation matrices r can optionally include applying a transform based at least on the angle.

BRIEF DESCRIPTION OF THE DRAWINGS

The present teachings will be more readily understood by reference to the following description, taken with the accompanying drawings, in which:

FIGS. **1**A and **1**B are flowcharts of the process of the present teachings;

FIG. **2** is a schematic block diagram of the system of the present teachings;

FIG. **2**A is a top view of an exemplary system indicating the fields of view of the cameras of the present teachings;

FIG. **2**B is a pictorial representation of a camera configuration that can supply data to the system of the present teachings;

FIGS. **3**A and **3**B are pictorial representations of the data processing steps of the present teachings;

FIGS. **4**A-**4**D are perspective diagrams of an exemplary sensor configuration of the present teachings; and

FIGS. **5**A-**5**C are flowcharts of a camera processing method of the present teachings.

DETAILED DESCRIPTION

The system and method of the present teachings can estimate the free space surrounding an autonomous vehicle in real time.

Referring now to FIG. **1**A, free space can be estimated by synchronizing and fusing data, and generating grid maps with occupancy and classification layers. Method **1250** for estimating free space around an autonomous vehicle can include, but is not limited to including, receiving **1251** camera image data and point cloud data into the autonomous vehicle, and semantically classifying **1253** each the image data based on a machine learning model, forming point classifications and point classification probabilities. Semantically classifying the image data can include developing, training, and evaluating a semantic segmentation model for real-time object detection. Such models can be acquired commercially, or they can be developed, or modifications can be made to commercial products. Commercial models can include, but are not limited to including, the ICNET semantic segmentation model in Keras with Tensorflow backend for detection of drivable surfaces, where the drivable surfaces can include, but are not limited to, road, sidewalk, ground, terrain surfaces, and lane markings.

Continuing to refer to FIG. **1**A, method **1250** can include associating **1255** each point in the point cloud data with the image data that are spatially co-located with the point cloud data, and performing **1257** a first transform on the points in the point cloud data into an image coordinate system associated with the image data. Associating each point in the point cloud data with the image data can include receiving the image data at a pre-selected rate, and mapping the point cloud data onto the image data. The image data can be collected by commercial cameras, and those cameras can provide image data through, for example, but not limited to, a MIPI interface. In some configurations, the cameras can stream data as a Robot Operating System (ROS) topic at a pre-selected resolution, for example, but not limited to, 2180×720, and for 360° centered at the autonomous device.

Continuing to refer to FIG. **1**A, method **1250** can include classifying **1259** each of the first transformed points that represents an obstructed space and the non-obstructed space based on a spatial association of the first transformed points with the semantically classified image data forming obstructed points and non-obstructed points, and performing **1261** a second transform on the first transformed points into a robot coordinate system associated with the autonomous vehicle. Point cloud data can be mapped onto the image data, and then further mapped to 3D coordinates of the base layer of the autonomous device.

Referring now to FIG. **1**B, method **1250** can include classifying **1263** each of the second transformed points that represents a non-obstructed space and an obstructed space within a pre-selected area surrounding the autonomous vehicle, forming a grid of obstructed and non-obstructed space, based on spatial association of the first transformed points with the semantically classified image data having the point classifications and the point probabilities. Non-obstructed space can be defined as any space that is not part of the obstructed space. Method **1250** can include associating **1265** the obstructed points with a first probability based at least on (a) noise in the point cloud data, (b) a second probability that the point cloud data are reliable, and (c) a third probability that the point classifications are correct. Method **1250** can include estimating **1267** the free space in the pre-selected area by computing a fourth probability based at least on (a) noise in the point cloud data, (b) the second probability, (c) the distance from the non-obstructed points to the obstructed space closest to the non-obstructed points, (4) the third probability, and (e) a presence of the non-obstructed space.

Referring now to FIG. **2**, system **200** for estimating free space around an autonomous vehicle can include, but is not limited to including, pre-processor **207** and free space estimator **202**. Pre-processor **207** can include receiving camera image data **218** from 3D cameras **201**A-**201***n*, referred to collectively as cameras **201**, and a synchronizer that can time-synchronize cameras **201** to each other. Some configurations can include three of 3D cameras **201**. Cameras **201** can include, but are not limited to including, MIPI cameras that can stream data at about 1280×720 resolution at about 30 Hz, and can be mounted on autonomous vehicle **121** (FIG. **3**A) to provide 360° perception around autonomous vehicle **121** (FIG. **3**A). Image data **218** can be semantically classified into classifications **215**, where classifications **215** can be based on the training received by a machine learning model executing in pre-processor **207**. The machine learning model can include a commercially-available semantic segmentation model trained for detecting specific types of features such as, for example, but not limited to, types of surfaces. Classes **215** of surfaces can include, but are not limited to including, road, sidewalk, ground, terrain surfaces, and lane markings. Lane markings can include white or yellow painted markings on the road, including solid white lines, broken white lines, yellow lines and cross walks, to indicate traffic traveling in the direction of the autonomous vehicle.

Continuing to refer to FIG. **2**, pre-processor **207** can provide image data **211**, classes **215**, point cloud data **213** from, for example, LIDAR **203**, and transforms **221** to synchronizer **216**. Synchronizer **216** can time-synchronize point cloud data **213**, transform data **221**, classes **215**, and images **211**. In some configurations, synchronizer **216** can create a ROS synchronized subscriber that can insure that any data that are received simultaneously have the same time stamp. The time stamp can mark the moment of the first data point of the first data block from the sensors and/or the transform data. In some configurations, synchronizer **216** can access a commercially-available filter that can synchronize incoming data by the timestamps contained in their headers, according to either exact time or approximate time. Exact time requires the data to have exactly the same time stamps in order to match. Approximate time can use, for example, hut not limited to, an adaptive algorithm to match data based on the time stamps of the data. A description of one such adaptive algorithm can be found at http://wiki.ros.org/message_filters/ApproximateTime.

Continuing to refer to FIG. **2**, free space estimator **202** can include 3D-point cloud to 3D image processor **225** that can include receiving synchronized image data **211**A at a pre-selected rate, and mapping point cloud data **213** onto image data **211**, which includes a spatial association of points to the cameras. 3D-point cloud to 3D image processor **225** can include associating each point in synchronized point cloud data **213**A with synchronized image data **211**A that are spatially co-located with synchronized point cloud data **213**A, and performing a first transform on synchronized point cloud data **213**A into an image coordinate system associated with synchronized image data **211**A. Associating each point (X,Y,Z) **111** (FIG. **3**A) in synchronized point cloud data **213**A with synchronized image data **211**A can include for each point (X,Y,Z) **111** (FIG. **3**A) in synchronized point cloud data **213**A, calculating angle α **122** that point (X,Y,Z) **111** (FIG. **3**A) subtends with center **117** (FIG. **3**A) of synchronized point cloud data **213**A as follows:

$X>0$ and $Y>0 \Rightarrow \alpha=0°+\text{atan}(Y/X)$ degrees$*180/\pi$
$X<0$ and $Y>0 \Rightarrow \alpha=90°-\text{atan}(X/Y)$ degrees$*180/\pi$
$X<0$ and $Y<0 \Rightarrow \alpha=180°+\text{atan}(Y/X)$ degrees$*180/\pi$
$X>0$ and $Y<0 \Rightarrow \alpha=270°-\text{atan}(X/Y)$ degrees$*180/\pi$

Angle α **122** indicates the field of view of one of cameras **201**. The field of view dictates which camera's semantic segmentation output image that point (X,Y,Z) **111** (FIG. **3**A) is mapped onto as follows:

$312°<\alpha\leq 360°$ or $48°\geq\alpha>0° \Rightarrow$ point mapped onto semantic segmentation output image derived from front camera **401** (FIG. **2**A);
$48°<\alpha<180° \Rightarrow$ point mapped onto semantic segmentation output image derived from left camera **403** (FIG. **2**A);
$180°<\alpha\leq 312° \Rightarrow$ point mapped onto semantic segmentation output image derived from right camera **405**A (FIG. **2**A).

PC/image grid **115**R/L/F (a grid for each camera) can result from the computations of 3D PC ➔ 3D image associator **225**.

Continuing to refer to FIG. **2**, 3D image to 2D RGB transform **227** can include projecting each mapped point onto a 2D image of a pre-selected size, for example, but not limited to, 1920×1080 to obtain X_{GRB}, Y_{GRB} pixel location **111** (FIG. **3**B). Because more than one mapped point could have the same X_{GRB}, Y_{GRB} pixel location **111** (FIG. **2**B), each projected X_{GRB}, Y_{GRB} pixel location **111** (FIG. **3**B) can be populated with a depth of a mapped point that is closest to autonomous vehicle **121** (FIG. **3**B). 3D image to 2D RGB transform **227** can include identifying each of the first transformed points that represents an obstructed space and a non-obstructed space based on a spatial association of the first transformed points with the semantically classified image data **211**A. The identified points can be termed obstructed points and non-obstructed points. 2D RGB data **116** can result from the computations of 3D image=>2D RGB transform **227**.

Continuing to refer to FIG. **2**, synchronized point cloud data **213**A can be mapped onto synchronized image data **211**A, and then further mapped to 3D coordinates of autonomous device **121**. 2D to 3D baselink transform **229** can include performing a second transform on the first transformed points into robot coordinate system points (X_{bl}, Y_{bl}, Z_{bl}) associated with autonomous vehicle **121** (FIG. **3**A) by a process relying on synchronized transforms **221**A provided by transform manager **205**. Synchronized classes **215**A are also provided to free space estimator **202**. 3D baselink to grid transform **231** can flatten robot coordinate system 3-D points (X_{bl}, Y_{bl}, Z_{bl}) to a 2D grid map surrounding autonomous device **121** (FIG. **3**B) that can extend to a pre-selected radius, for example, but not limited to, 20 m. Cell **131** (FIG. **3**B) in grid map **133** (FIG. **3**B) can by identified as occupied if the semantic segmentation output also confirms that points in cell **131** (FIG. **3**B) correspond to an obstructed space. Point (X_{RGB}, Y_{RGB}) **111** (FIG. **3**B) in semantic segmentation's output image can include values such as, but not limited to, 0=non-drivable, 1=road, 2=sidewalk, 3=terrain, 4=lane marking, and thus, >0=drivable, 0=obstructed. Obstructed space or non-drivable surfaces can include surfaces that are impassable by a wheelchair/bicycle/car sized vehicle. 3D baselink data **132** can result from the computations of 2D RGB=>3D baselink transform **229**.

Continuing to refer to FIG. **2**, layer processor **233** can include classifying each of the second transformed points that represents a non-obstructed space and an obstructed space within a pre-selected area surrounding autonomous vehicle **121**, forming a grid of obstructed and non-obstructed space, based on a spatial association of the first transformed points with the semantically classified image data having the point classifications and the point probabilities. Layer processor **233** can include associating the obstructed points with a first probability based at least on (a) noise in the point cloud data, (b) a second probability that the point cloud data are reliable, and (c) a third probability that the point classifications are correct. Layer processor **233** can include estimating the free space in the pre-selected area by computing a fourth probability based at least on (1) noise in the point cloud data, (2) the second probability, (3) the distance from the non-obstructed points to the obstructed space closest to the non-obstructed points, (4) the third probability, and (5) presence of non-obstructed space.

Continuing to refer to FIG. **2**, after the process described herein is complete, grid map **133** includes obstructed spaces classifications, probabilities, and probability log odds. Free space can be determined by extending line **125** (FIG. **3**B) from center **121**A (FIG. **3**B) of grid map **133** (FIG. **3**B) to end-point **121**B (FIG. **3**B) on the boundary of the pre-selected area surrounding autonomous vehicle **121** (FIG. **3**B). Along line **125** (FIG. **3**B), cells **131** (FIG. **3**B) that are not obstructed in grid

map **133** (FIG. **3**B) between blind area **123** (FIG. **3**B) and the last of cells **131** (FIG. **3**B) that is not obstructed or end-point **121**B (FIG. **3**B) can be marked as free space. Each can be associated with a Gaussian probability that marked cell is actually a free space. Blind area **123** (FIG. **3**B) is an area surrounding LIDAR **117** (FIG. **2**) where data cannot be gathered.

Referring now to FIGS. **2**A and **2**B, in some configurations, three long-range cameras, **201**L, **201**F, and **201**R, can provide fields of view **410**, **412**, **414**, respectively, that can together provide a 360° field of view. The field of view may be defined by camera selection, the number of cameras, and by the location of the cameras within camera assembly **400**. In describing fields of view herein, the zero angle can be a ray located in a vertical plain through the center of the autonomous vehicle **121** (FIG. **3**B) and perpendicular to the front of autonomous vehicle **121** (FIG. **3**B). The zero angle ray can pass through the front of autonomous vehicle **121**. Front camera located **201**F can have a 96° field of view **412** from 312° to 360° and 0° to 48°. Left side camera **201**L can have a field of view **410** from 48° to 180°. Right side camera **201**R can have a field of view **414** from 180° to 312°.

Referring now to FIGS. **4**A-**4**D, in some configurations, LIDAR **420** can provide a 360° horizontal field of view around autonomous vehicle **121** (FIG. **3**B). In some configurations, the vertical field of view is 40° and, for example, mounted at 1.2 meters above the ground, can set the minimum distance at which LIDAR **420** can detect data at about four meters from autonomous vehicle **121** (FIG. **3**B). Sensor assembly **400** can include cover **430** to protect assembly electronics from wear and tear. LIDAR **420** can provide data on the range or distance to surfaces around autonomous vehicle **121** (FIG. **3**B). In some configurations, processor **470** can processor the data from LIDAR **420**. LIDAR **420** can be mounted on structure **405** above cameras **440**A-C and cover **430**. LIDAR **420** is one example of a ranging sensor based on reflected laser pulsed light. The invention encompasses other ranging sensors such as radar which uses reflected radio waves. In one example, LIDAR **420** is the Puck sensor by VELODYNE LIDAR®.

Continuing to refer to FIGS. **4**A-**4**D, cameras **440**A, **440**B, **440**C can provide digital images of objects, surfaces and structures around autonomous vehicle **121** (FIG. **3**B). Cameras **440**A, **440**B, **440**C can receive images through windows **434**, **436** and **438** that are mounted in cover **430**. Cameras **440**A, **440**B, **440**C can include various kinds of lenses including, but not limited to, fisheye lens **442** (FIG. **4**D) camera **444**. Fisheye lens **442** can expand the field of view of camera **444** up to, for example, 180°. In some configurations, camera **444** can include a camera similar to e-cam52A_56540_MOD by E-con Systems of San Jose Calif. In some configurations, fisheye lens **442** can include a lens similar to model DSL227 by Sunex of Carlsbad, Calif. Cameras **440**A, **440**B, **440**C can be arranged around structure **405** with respect to cover **430** to fields of view that cover the entire 360° around autonomous vehicle **121** (FIG. **3**B).

Continuing to refer to FIGS. **4**A-**4**D, mounting sensor assembly **400** on top of autonomous vehicle **121** (FIG. **3**B) can free the sensors of blocking by nearby objects including, but not limited to, people, cars, and low walls. Mounting sensor assembly **400** to the top of autonomous vehicle **121** (FIG. **3**B) can provide a substantial and rigid mount that can resist deflections that can be caused by, for example, but not limited to, movement of autonomous vehicle **121** (FIG. **3**B). Cover **430** can be sealed from the weather by, for example, but not limited to, an O-Ring between cover **430** and the top of autonomous vehicle **121** (FIG. **3**B).

Referring now to FIGS. **5**A-**5**C, method **150** for mapping LIDAR 3D points onto semantically segmented images from multiple cameras can include, but is not limited to including, accessing **151** semantically segmented image data and point cloud data, and accessing **153** a ROS synchronized subscriber that can insure that any data that are received simultaneously have the same time stamp as described herein. The method can include receiving time-synchronized LIDAR points and three images that are outputs from semantic segmentation corresponding to cameras mounted on the front, and to the left and right of the front camera, on a robot, and rotating LIDAR points from the LIDAR coordinate system to the image coordinate system of the cameras. The rotation step produces rotated points in a 3D frame of reference according to a LIDAR image rotation matrix R by applying a roll of −90° and a yaw of −90°. The rotation step can further include applying the rotation matrix R and camera translation factors $t_x/t_y/t_z$ to each of the rotated LIDAR points, to convert the aligned LIDAR points to 3D image points, applying camera rotation matrices r to each of the LIDAR points to align the LIDAR frame with the camera frame, arriving at x/y/z, projecting matrix K from calibration of the cameras, applying the projection matrix K to the 3D image points, arriving at x/y/z, and therefore converting the 3D image points to 2D points: X_{rgb}=x/z, Y_{rgb}=y/z. Because more than one LIDAR point may have same X_{rgb}, Y_{rgb} values, each projected 2D value X_{rgb}, Y_{rgb} in the image is populated with the depth of a LIDAR point that is closest to autonomous vehicle **121** (FIG. **3**A). In some configurations, the 2D image can include 1920×1080 pixels.

Continuing to refer to FIGS. **5**A-**5**C, method **150** can optionally include wherein computing the LIDAR image rotation R can include, but is not limited to including, computing Euler and Tait-Bryan rotations as combinations of 3-axis rotations (R_x, R_y, R_z). The combined rotation matrix is a product of two or three of the $R_x/R_y/R_z$ matrices.

Continuing to refer to FIGS. **5**A-**5**C, method **150** can include determining the rotation matrices r that can include, but is not limited to including, for each point (X, Y, Z) in the LIDAR point cloud, calculating angle **122** (FIG. **3**A) that point **111** (FIG. **3**A) subtends with the center of LIDAR **117** (FIG. **3**A). If **155** there are more points to process, and if **157** X>0 and Y>0, set **159** angle **122** (FIG. **3**A)=0°+atan (Y/X)*180/π. If **161** X<0 and Y>0, set **163** angle **122** (FIG. **3**A)=90°−atan (X/Y)*180/π. If **165** X<0 and Y<0, set **167** angle **122** (FIG. **3**A)=180°+atan (Y/X)*180/π. If **169** X>0 and Y<0, set **171** angle **122** (FIG. **3**A)=270°−atan (X/Y)*180/π, otherwise error out **185**. Method **150** can include if **173** angle **122** (FIG. **3**A) is between 0° and 48° or angle **122** (FIG. **3**A) is between 312° and 360°, mapping **175** point **111** (FIG. **3**A) onto the semantic segmentation output image derived from front camera **201**A (FIG. **2**B). Method **150** can include if **177** angle **122** (FIG. **3**A) is between 48° and 180°, mapping **179** point **111** (FIG. **3**A) onto the semantic segmentation output image derived from left camera **201**B (FIG. **2**B). Method **150** includes if **181** angle **122** (FIG. **3**A) is between 180° and 312°, mapping **183** point **111** (FIG. **3**A) onto the semantic segmentation output image derived from right camera **201**C (FIG. **2**B). Angle **122** (FIG. **3**A) indicates that point **111** (FIG. **3**A) falls into the field of view one of cameras **201** (FIG. **2**). Transform matrices **221** (FIG. **2**) can differ depending upon which of cameras **201** (FIG. **2**) that point **111** (FIG. **3**A) is mapped.

Configurations of the present teachings are directed to computer systems for accomplishing the methods discussed in the description herein, and to computer readable media containing programs for accomplishing these methods. The raw data and results can be stored for future retrieval and processing, printed, displayed, transferred to another computer, and/or transferred elsewhere. Communications links can be wired or wireless, for example, using cellular communication systems, military communications systems, and satellite communications systems. Parts of the system can operate on a computer having a variable number of CPUs. Other alternative computer platforms can be used.

The present configuration is also directed to software for accomplishing the methods discussed herein, and computer readable media storing software for accomplishing these methods. The various modules described herein can be accomplished on the same CPU, or can be accomplished on different computers. In compliance with the statute, the present configuration has been described in language more or less specific as to structural and methodical features. It is to be understood, however, that the present configuration is not limited to the specific features shown and described, since the means herein disclosed comprise preferred forms of putting the present configuration into effect.

Methods can be, in whole or in part, implemented electronically. Signals representing actions taken by elements of the system and other disclosed configurations can travel over at least one live communications network. Control and data information can be electronically executed and stored on at least one computer-readable medium. The system can be implemented to execute on at least one computer node in at least one live communications network. Common forms of at least one computer-readable medium can include, for example, but not be limited to, a floppy disk, a flexible disk, a hard disk, magnetic tape, or any other magnetic medium, a compact disk read only memory or any other optical medium, punched cards, paper tape, or any other physical medium with patterns of holes, a random access memory, a programmable read only memory, and erasable programmable read only memory (EPROM), a Flash EPROM, or any other memory chip or cartridge, or any other medium from which a computer can read. Further, the at least one computer readable medium can contain graphs in any form, subject to appropriate licenses where necessary, including, but not limited to, Graphic Interchange Format (GIF), Joint Photographic Experts Group (JPEG), Portable Network Graphics (PNG), Scalable Vector Graphics (SVG), and Tagged Image File Format (TIFF).

While the present teachings have been described above in terms of specific configurations, it is to be understood that they are not limited to these disclosed configurations. Many modifications and other configurations will come to mind to those skilled in the art to which this pertains, and which are intended to be and are covered by both this disclosure and the appended claims. It is intended that the scope of the present teachings should be determined by proper interpretation and construction of the appended claims and their legal equivalents, as understood by those of skill in the art relying upon the disclosure in this specification and the attached drawings.

What is claimed is:

1. A method for estimating free space based on image data and point cloud data, the free space used for navigating an autonomous vehicle, the method comprising:

semantically classifying the image data based on a machine learning model forming point classifications and point classification probabilities;

associating each point in the point cloud data to the image data that are spatially co-located with the point cloud data;

classifying each of the points as an obstructed space or a non-obstructed space based on the spatial association of each of the points with the semantically classified image data forming obstructed points and non-obstructed points;

forming a grid of the obstructed points and non-obstructed points within a pre-selected area surrounding the autonomous vehicle; and

estimating the free space in the pre-selected area by associating the obstructed points with a first probability based at least on (1) noise in the point cloud data, (2) a second probability that the point cloud data are reliable, (3) a distance from the non-obstructed points to the obstructed space closest to the non-obstructed points, (4) a third probability that the point classifications are correct, and (5) presence of the non-obstructed space.

2. The method as in claim **1** further comprising:

receiving the image data and the point cloud data into the autonomous vehicle.

3. The method as in claim **1** further comprising:

performing a first transform on the points in the point cloud data into an image coordinate system associated with the image data.

4. The method as in claim **3** further comprising:

performing a second transform on the first transformed points into a robot coordinate system associated with the autonomous vehicle.

5. The method as in claim **1** wherein the image data comprise streaming data from a pre-selected number of at least one camera, the at least one camera providing a 360° view of an area surrounding the autonomous vehicle.

6. The method as in claim **1** wherein the machine learning model comprises an ICNET semantic segmentation model.

7. The method as in claim **1** wherein the machine learning model comprises detecting at least one drivable surface.

8. The method as in claim **7** wherein the at least one drivable surface is selected from a group consisting of road, sidewalk, ground, terrain surfaces, and lane markings.

9. The method as in claim **1** wherein the associating each point comprises:

receiving the image data at a pre-selected rate; and

mapping the point cloud data onto the image data.

10. A system for estimating free space based on image data and point cloud data, the free space used for navigating an autonomous vehicle, the autonomous vehicle having a front, a left side, and a right side, the system comprising:

a pre-processor configured to receive camera image data from at least one camera, the pre-processor configured to semantically classify each pixel of the image data into a classification and calculate a probability associated with the classification, the classification and the probability being determined by a machine learning model; and

a free space estimator configured to compute an obstacle classification layer, a probability layer, and a log odds layer based on the point cloud data and the image data;

wherein the free space estimator comprises:

a 3D point cloud to 3D image processor configured to transform the 3D point cloud to 3D image coordinates;

a 3D image to 2D RGB transform configured to transform the 3D image coordinates to 2D RGB coordinates; and

a 2D to 3D baselink transform configured to transform the 2D RGB coordinates to 3D baselink coordinates forming transformed point cloud data.

11. The system as in claim **10** wherein the camera image data comprises streaming data from the at least one camera, the at least one camera providing a 360° view of an area surrounding the autonomous vehicle.

12. The system as in claim **10** wherein a number of the at least one camera comprises three cameras.

13. The system as in claim **10** wherein the machine learning model is configured to detect drivable surfaces, the drivable surfaces including lane markings.

14. The system as in claim **10** wherein the free space estimator is configured to receive data having time stamps into a synchronizer, the synchronizer time-synchronizing the point cloud data, the transformed point cloud data, and the classification based on the time stamps.

15. The system as in claim **10** wherein the 3D point cloud to 3D image processor comprises:

receiving the point cloud data from at least one LIDAR sensor, the classification and the probability of each point of the point cloud data, and coordinate transforms;

associating each of the points in the point cloud data to the image data that are spatially co-located with the point cloud data; and

performing a first transform on the points in the point cloud data into an image coordinate system associated with the image data.

16. The system as in claim **15** wherein associating each point in synchronized point cloud data with a synchronized image data comprises:

for each of the points (X,Y,Z) in the synchronized point cloud data, calculating an angle that the point subtends with a center of the synchronized point cloud data, the angle indicating a field of view of the at least one camera, the calculating including:

if X>0 and Y>0 then the angle=0°+atan(Y/X) degrees*180/π;

if X<0 and Y>0 then the angle=90°−atan(X/Y) degrees*180/π;

if X<0 and Y<0 then the angle=180°+atan(Y/X) degrees*180/π; and

if X>0 and Y<0 then the angle=270°−atan(X/Y) degrees*180/π;

mapping each of the points onto a semantic segmentation output image including:

if 312°<the angle≤360° or 48°≥the angle>0° then mapping the point onto the semantic segmentation output image derived from the at least one camera located at the front of the autonomous vehicle;

if 48°<the angle<180° then mapping the point onto the semantic segmentation output image derived from the at least one camera located on the left side; and

if 180°<the angle≤312° then mapping the point onto the semantic segmentation output image derived from the at least one camera located on the right side.

17. The system as in claim **10** wherein the 3D image to 2D RGB transform comprises:

identifying each of the points that represents an obstructed space and a non-obstructed space based on a spatial association of the points with the semantically classified image data.

18. The system as in claim **16** wherein the 2D to 3D baselink transform comprises performing a transform on the points into a robot coordinate system associated with the autonomous vehicle.

19. The system as in claim **18** wherein the 3D baselink to grid transform comprises:

flattening robot coordinate system points (Xbl, Ybl, Zbl) to a 2D grid map surrounding the autonomous vehicle, the 2D grid map extending to a pre-selected radius around the autonomous vehicle; and

identifying at least one cell of the 2D grid map as occupied if a semantic segmentation output point (XRGB, YRGB), of the semantic segmentation output image, spatially associated with the at least one cell corresponds to an obstructed space.

20. The system as in claim **19** wherein the semantic segmentation output point (XRGB, YRGB) comprises values including 0=non-drivable, 1=road, 2=sidewalk, 3=terrain, 4=lane marking, >0=drivable, 0=obstructed.

21. The system as in claim **19** further comprising:

a layer processor configured to

classify each of the points that represents a non-obstructed space and an obstructed space within a pre-selected area surrounding the autonomous vehicle, form a spatial grid of obstructed points and non-obstructed points, based on spatial association of the points with the semantically classified image data having point classifications and point probabilities; and

estimate the free space in the pre-selected area by associating the obstructed points with a first probability based at least on (1) noise in the point cloud data, (2) a second probability that the point cloud data are reliable, (3) a distance from the non-obstructed points to the obstructed points closest to the non-obstructed points, (4) a third probability that the point classifications are correct, and (5) presence of the non-obstructed points.

22. The system as in claim **21** wherein the non-obstructed space comprises space that is not part of the obstructed space.

23. The system as in claim **21** wherein the layer processor comprises:

estimating the free space by extending a line from a grid map center of the grid map to a boundary of the pre-selected area; and

along the line, marking the free space as the at least one cell that is not the obstructed space in the grid map between a blind area and a last free space present in the line.

24. The system as in claim **23** wherein the blind area comprises an area surrounding the at least one LIDAR sensor where the point cloud data cannot be gathered.

25. A system for estimating free space based on image data and point cloud data, the free space used for navigating an autonomous vehicle, the autonomous vehicle having a front, a left side, and a right side, the system comprising:

a pre-processor configured to receive camera image data from at least one camera, the pre-processor configured to semantically classify each pixel of the image data into a classification and calculating a probability associated with the classification, the classification and the probability being determined by a machine learning model; and

a free space estimator configured to compute an obstacle classification layer, a probability layer, and a log odds layer based on the point cloud data and the image data;

wherein the free space estimator comprises:

- a 3D point cloud to 3D image processor configured to transform the 3D point cloud to 3D image coordinates; and
- a 3D image to 2D RGB transform configured to transform the 3D image coordinates to 2D RGB coordinates; and

wherein the 3D image to 2D RGB transform comprises identifying each of the points that represents an obstructed space and a non-obstructed space based on a spatial association of the points with the semantically classified image data.

* * * * *